

## Original Article

# Huiyang Shengji Extract improved wound healing by regulating macrophage phenotype transition

Xiujuan He, Yan Lin, Yujiao Meng, Yan Xue, Xuyang Han, Ping Li

Beijing Institute of TCM, Beijing Hospital of Traditional Chinese Medicine, Capital Medical University, Beijing, P. R. China

Received March 7, 2018; Accepted July 14, 2018; Epub November 15, 2018; Published November 30, 2018

**Abstract:** Dysfunction of macrophage phenotype transition is a primary reason for wound healing failure caused by persistent inflammation. Huiyang Shengji Extract (HSE) is a Traditional Chinese Medicine prescription for treating chronic wounds. Little is known about the underlying molecular mechanism of HSE. This study aim to investigate the effect of HSE on macrophage phenotype transition in chronic skin wound of mice and macrophages *in vitro*. Balb/c mice were randomly divided into four groups: control (normal wound-NS treated), model (delayed wound-NS treated), HSE-treated groups, and bFGF-treated groups. The immunosuppressive mice were operated by full-thickness excision. Macrophage phenotype markers on the wound were analyzed by immunohistochemistry, real-time PCR, and Western blot. The *in vitro* cytotoxicity and phagocytosis of macrophages was assessed by CCK-8 and neutral red assays. Macrophage 1/2 (M1/M2) markers were analyzed using ELISA, flow cytometry, and real-time PCR. The results showed delayed wound healing in immunosuppressed mice. HSE promoted macrophage recruitment to the wounded tissue, decreased the expression of iNOS and IL-6, and increased the level of CD206, VEGF, and TGF- $\beta$  during granulation tissue formation. *In vitro*, HSE inhibited the inflammatory activated macrophages secreting M1 cytokines, promoted secretion of M2 cytokines, increased Arg-1 mRNA, and decreased iNOS mRNA significantly. In conclusion, an imbalance of macrophage phenotype contributed to impaired wound healing in immunosuppressed mice. HSE promoted impaired wound healing by regulating the macrophage phenotype transition: a potential therapeutic mechanism of HSE for the chronic non-healing wound.

**Keywords:** Delayed wound healing, Traditional Chinese Medicine, macrophage phenotype, Huiyang Shengji Extract

## Introduction

Chronic non-healing cutaneous wounds, such as diabetic foot ulcers, venous leg ulcer, pressure skin ulcer, and nutritional deficiency ulcers, affect the life of patients and cause an economic burden to the society [1-4]. The pathological characteristic of a non-healing wound is persistent inflammation [5-7]. Recent studies have shown that dysfunction of wound macrophage phenotypic transformation is one of the primary reasons for healing failure caused by persistent inflammation [8, 9]. Pro-inflammatory M1 macrophages (classically activated M1 macrophages) release high concentrations of pro-inflammatory cytokines (TNF- $\alpha$ , IL-1 $\beta$ , IL-6, and IL-12) and inducible nitric oxide synthase (iNOS) in the inflammatory phase. Pro-healing M2 macrophages (alternatively activated M2 macrophages) produce anti-inflammatory cytokine (IL-10), growth factors (TGF- $\beta$ 1, VEGF, and

PDGF), ECM, and arginase-1 (Arg-1) in granulation tissue formation phase [10]. Wound M1 macrophages transiting successfully to M2 macrophages are indicative of inflammatory phase transition into granulation tissue formation phase [11, 12]. The persistence of an unrestrained M1 macrophage population with an incomplete switch to an M2 phenotype has been shown as a typical characteristic of non-healing wounds such as chronic venous leg ulcers of humans and mice [13]. M1 macrophages with high expression of IL-1 $\beta$ , IL-6, TNF- $\alpha$ , and iNOS have been shown to persist through the late phases of wound healing of diabetic db/db mice [14]. Application of *ex vivo* generated M2 macrophages did not improve the murine healing response when polarized macrophages were injected into full-thickness excisional skin wounds of either C57BL/6 or diabetic db/db mice [15]. Therefore, regulating the macrophage phenotype switch of the wound may be a

# Huiyang Shengji Extract regulated macrophage phenotype transition

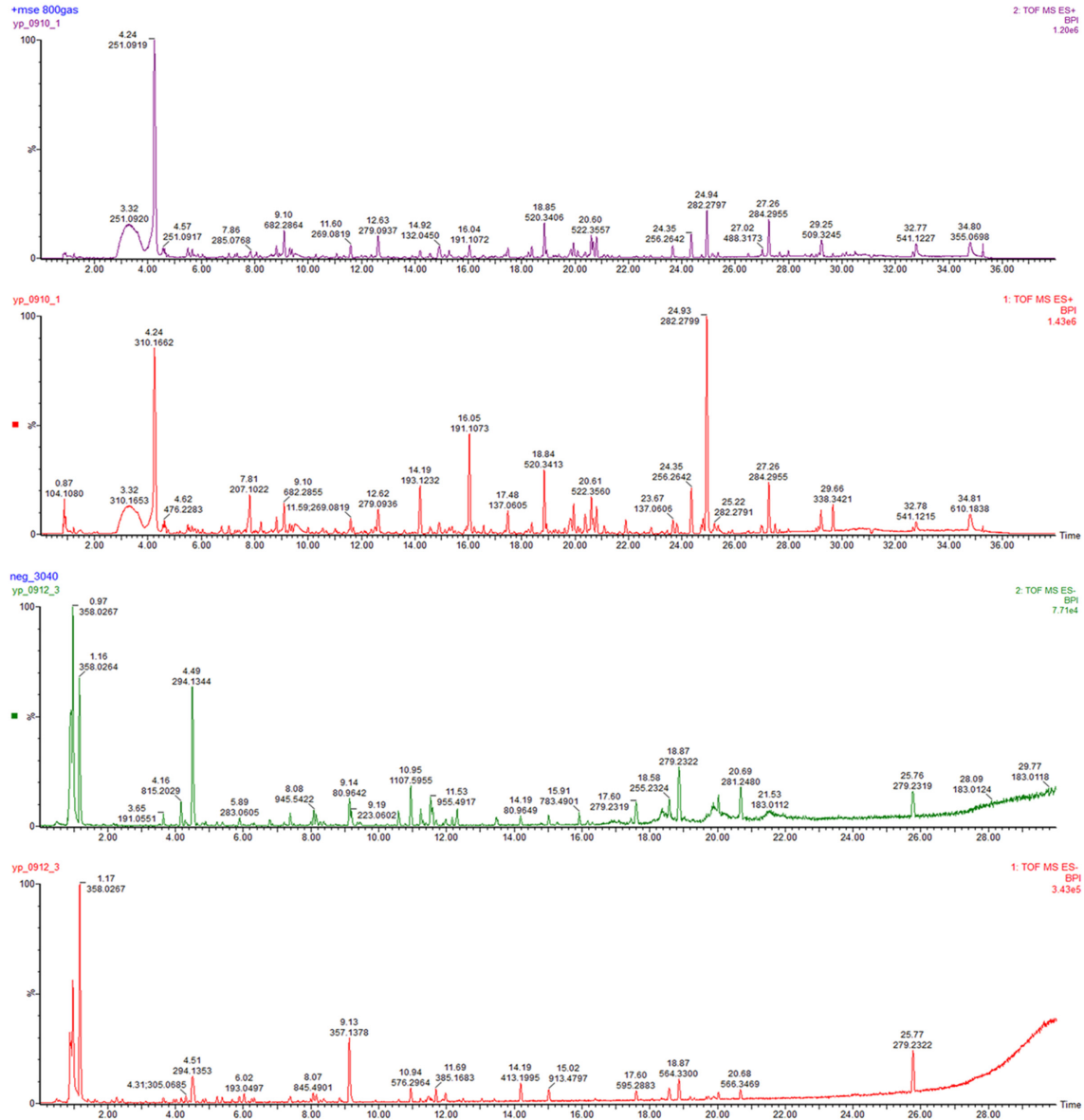


**Figure 1.** UPLC/Q-TOF-MSE profile of HSE.

novel therapeutic strategy to promote chronic wound healing [14, 16]. Alternative ways to modify the wound macrophages' phenotype into a pro-healing profile, by blocking pro-inflammatory factors such as IL-1 $\beta$  or TNF, have proven promising therapeutic approaches [14].

Huiyang Shengji Extract (HSE), Chinese herbal compound, is composed of Cinnamomi cortex (*Cinnamomum cassia* Presl, cortex), Ginseng radix et rhizome (*Panax ginseng* C.A.Mey., root and rhizome), Chuanxiong rhizoma (*Ligusticum chuanxiong* Hort., rhizome), Cervi cornu pantot-

richum (*Cervus nippon* Temminck or *Cervus elaphus* Linnaeus, young cornu) etc., (Editorial Committee of Pharmacopoeia of Ministry of Health P. R. China, 2010). It exhibits a satisfactory clinical effect in patients with the non-healing wound and has been produced and applied in Beijing Hospital of TCM for sixty years [17]. Our previous results showed that HSE accelerated normal human fibroblasts and ulcer margin fibroblasts proliferation by promoting more cells in the G0/G1 and S phase and up-regulation of nuclear transduction factor c-fos and c-myc expression [18, 19]. However, little is

# Huiyang Shengji Extract regulated macrophage phenotype transition

known about the underlying molecular mechanism of HSE.

In the present study, we aimed to investigate how HSE promotes chronic wound healing through regulation of wound macrophage phenotype transition in the impaired wound of hydrocortisone-induced immunosuppressive mice and activated macrophages by inflammation *in vitro*, providing experimental evidence for clinical application.

## Materials and methods

### Preparation of HSE

HSE powders were provided by Beijing Hospital of TCM, affiliated with Capital Medical University, (Beijing, China). The powder, composed of Cinnamomi cortex, Ginseng radix et rhizome, Chuanxiong rhizoma, Cervi cornu pan-totrichum etc., was immersed in 95% alcohol, followed by flash extraction with herbal blitzkrieg extractor (JHBE-50T, Henan Jinnai Tech. Co., Ltd), and centrifugation at 4000 rpm for 10 minutes. Then supernatant was decompressed and recycled in order to evaporate it to powder. The alcohol extract of HSE was used for *in vitro* experiments.

The above powder was solubilized in distilled water for 30 minutes, flash extracted for 30, 10, 10, and 10 seconds, centrifuged at 4000 rpm for 10 minutes, and the supernatant was boiled and condensed. The precipitate was solubilized in distilled water, flash extracted for 15, 15, 10, 10, and 10 seconds, and centrifuged. The supernatant is heated to boiling, condensed and dried in reduced pressure vacuum drying oven. These powders were alcohol extract-water extracting of HSE for animal experiments. HSE was solubilized in PBS, filtered, and stored at 4°C.

The chemical profile of HSE was established by ultra performance liquid chromatography coupled with quadrupole time-of-flight mass spectrometry (UPLC/Q-TOF-MS<sup>E</sup>) analysis (**Figure 1**). The ESI source was operated in the positive or negative ionization mode. The mass-scan range was 50-1500.

### Animals and grouping

Male Balb/c mice weighing 18-20 g (6 weeks of age) were commercially obtained from Beijing

HFk Bioscience Co. Ltd., China. The animals received humane care and were fed with standard mouse chow diet *ad libitum*. The animal experiments were approved by the Laboratory Animal Welfare Ethics Committee of Beijing Institute of TCM. The mice were allowed free access to a pellet diet and water and were housed in individual cages after wound operation. All methods were performed in accordance with the relevant guidelines and regulations.

Sixty animals were randomly divided into each of the following six groups with ten mice per group: control (normal wound-NS treated), model (delayed wound-NS treated), basic fibroblast growth factor (bFGF) groups (delayed wound-bFGF treated), and HSE groups with high/medium/low dose (delayed wound-HSE high/medium/low dose treatment). These groups were observed for wound healing time and healing rate with Image-Pro Plus6.0 software on day 0, 7, and 14 after wounding. The animals with delayed wound were treated by intramuscular injection of hydrocortisone (0.5 mg/d, Tianjin Jinyao Amino Acid Co. Ltd., China) for 7 days [20, 21], and the control group received normal saline (NS). The mice were then anesthetized by intraperitoneal injection of pentobarbital sodium (60 mg/kg). The dorsal surface of the experimental mice was shaved and sterilized, and a 7 mm diameter full-thickness wound was operated with a biopsy punch. Subsequently, the delayed wound group was treated by intramuscular injection of hydrocortisone (0.25 mg/d) every other day, and the control group received NS. The HSE groups were externally treated with HSE (50 µL) with a high dose (0.036 g/cm<sup>2</sup>), medium dose (0.018 g/cm<sup>2</sup>-equivalent to the clinical dose), and low dose (0.009 g/cm<sup>2</sup>) on an absorbable gelatin sponge (1 cm<sup>2</sup>, Xiang'en Medical Technology Development Co. Ltd., China). The model and control groups were both treated with N.S (50 µL). The bFGF group was treated with bFGF (50 µL, 90 AU/cm<sup>2</sup>, PeproTech, USA) on the same sponge. Transparent semipermeable dressings (Shandong dermcosy medical co., Ltd, China) were applied over the gelatin sponge. The external medicine and dressing were changed every other day until 14 days (**Figure 2**). Next, one hundred and twenty mice were randomly divided into the following four groups with thirty animals per group: control, model, HSE-L (0.009

## Huiyang Shengji Extract regulated macrophage phenotype transition

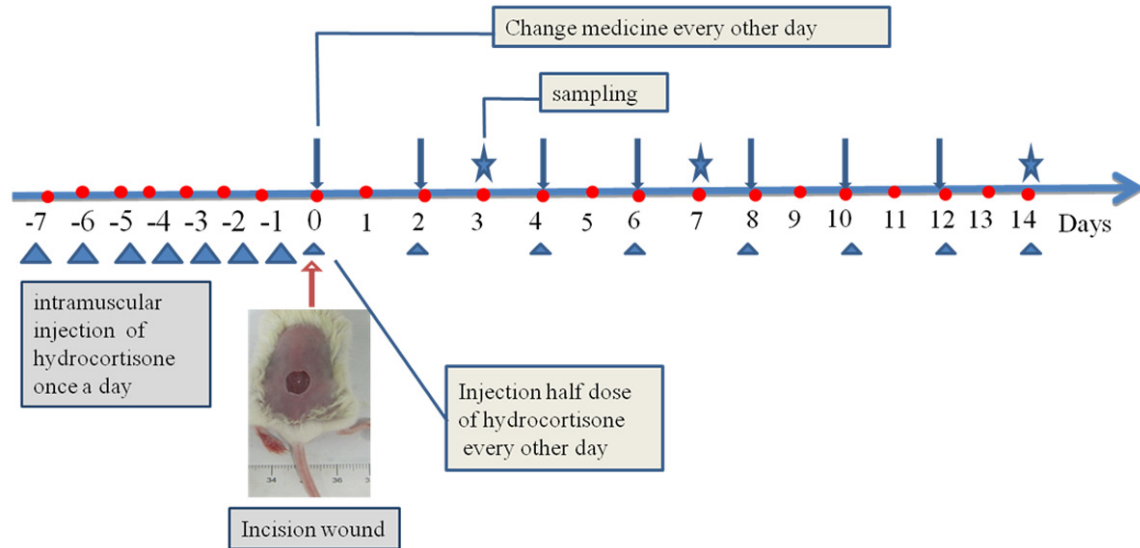


**Figure 2.** Schematic of immunosuppressive mice with skin ulcer. The animals of the model group were treated by intramuscular injection of hydrocortisone for 7 days (0.5 mg/d), and the control group received normal saline. A 7 mm diameter full-thickness wound was operated on the backs of mice with a biopsy punch. Subsequently, the delayed wound group was treated by half dose of hydrocortisone every other day, and the control group received NS. The delayed wound of mice was externally treated with HSE (high/medium/low dose), bFGF and NS separately on an absorbable gelatin sponge, which were covered by transparent semipermeable dressings. “▲”: intramuscular injection of hydrocortisone, “↓”: externally treatment with HSE/bFGF/NS, “★”: sampling.

g/cm<sup>2</sup>), and bFGF (90 AU/cm<sup>2</sup>) groups. Establishment of the animal model and medicine application as described above. The wounds were photographed by a digital camera on day 0, 2, 4, 6, 8, and 10. The wound healing rate = (original area - sampling wound area) / original area × 100%. At day 3, 7, and 14 post-wounding, the mice were sacrificed, and 0.5 mm skin tissue around the wound was harvested. The sliced samples were fixed in 10% formalin for HE, Masson staining, and immunohistochemistry. The remaining sections were prepared for real-time PCR (RT-PCR) and Western blot.

### Cell culture

Human acute monocytic leukemia cell line (THP-1) was purchased from the Institute of Basic Medical Cell Resource Center (Chinese Academy of Medical Sciences) and maintained at  $2 \times 10^5$  cells/mL in RPMI 1640 medium supplemented with 10% FCS and 2 mmol/L L-glutamine. THP-1 cells ( $2 \times 10^5$ /mL) became macrophages after stimulated with phorbol 12-myristate 13-acetate (PMA, 100 ng/mL, Sigma-Aldrich) for 24 hours. The macrophages were then incubated in fresh RPMI 1640 (10% FCS, 1% L-glutamine). The activity of the macrophages was tested with Cell Counting kit-8

(Dojindo Molecular Technologies Inc., Japan), and the phagocytic function was evaluated with neutral red dye assay.

The macrophages were activated by stimulation for 48 hours with LPS (100 ng/mL, Sigma) plus INF- $\gamma$  (40 ng/mL, BioLegend) for an inflammatory state [22]. Consequently, the macrophages were divided into the following six groups: normal, activated macrophages, lovastatin and HSE-high/middle/low dose group. Normal (PMA) and activated macrophage groups (PMA+LPS+INF- $\gamma$ ) were treated with RPMI 1640 medium, activated macrophages of HSE group were treated with HSE-high/middle/low dose (0.0016/0.00032/0.000064 g/L), and activated macrophages of lovastatin group were treated with lovastatin (10  $\mu$ mol/L, National Institutes for Food and Drug Control, China). The supernatants of the macrophages treated with HSE/lovastatin/RPMI 1640 for 24 hours were collected to test human TNF- $\alpha$ , IL-1 $\beta$ , IL-6, IL-10, IL-12, and VEGF with Cytometric Beads Array (Becton Dickinson and Co., USA), and TGF- $\beta$  with ELISA kit (eBioscience).

### Cell counting kit-8 assay

A total of 100  $\mu$ L of macrophage suspension (5000 cells/well) was dispensed in a 96-well

## Huiyang Shengji Extract regulated macrophage phenotype transition

**Table 1.** Primer sequences for targeted cDNAs

Primer	(5'-3') sequence (F: forward; R: reverse)	bp
TNF- $\alpha$	F: CTCTGTGAAGGGAATGGGTG R: GGGCTCTGAGGAGTAGACGATAAAG	94
IL-6	F: TCCTACCCCAATTTCCAATGCTCT R: ACCACAGTGAGGAATGTCCACAA	189
IL-12A	F: TCAACGCAGCACTTCAGAATCACAA R: GAAGGCGTGAAGCAGGATGCAGAGC	185
IL-10	F: CTGGACAACATACTGCTAACCGACTC R: AACTGGATCATTTCCGATAAGGC	86
TGF- $\beta$	F: GCCCTGGATACCAACTATTGCTTCA R: CAGAAGTTGGCATGGT	131
VEGF	F: TGTGCAGGCTGCTGTAACGATGA R: GTGCTGGCTTTGGTGAGGTTTGAT	212
ACTIN	F: GCCTTCTTCTTGGGTAT R: GGCATAGAGGTCTTTACGG	97
iNOS	F: TCATCCGCTATGCTGGCTAC R: CTCAGGGTCACGGCCATTG	161
Arg-1	F: GCCAAGTTATTGCAACTGCTGTG R: GAAATCTACAAAACAGGGCTACTCTCA	119
ACTIN	F: ACTTAGTTGCGTTACACCCTT R: GTCACCTTACCGTTCCA	156

plate. Then, 10  $\mu$ L of various concentrations of HSE and cultured in a humid chamber (37°C, 5% CO<sub>2</sub>) for 24 hours, followed by 10  $\mu$ L of the CCK-8 solution, incubated in a humid incubator for 4 hours. The absorbance was measured at 450 nm using a microplate reader.

### Neutral red dye assay

After treatment with HSE for 24 hours, the supernatant of macrophages was discarded, the neutral red dye was added, the cells were incubated in a humid incubator (37°C, 5% CO<sub>2</sub>) for 4 hours, washed with PBS twice, and then in pyrolysis liquid overnight. Microplate reader was used for detection.

### Cytometric beads array

Activated macrophages were treated with HSE/lovastatin/RPMI 1640 for 12 and 24 hours, the supernatant of macrophages was collected for the assay. Vortex the mixture of capture beads and add 50  $\mu$ L to all the assay tubes. Then, 50  $\mu$ L of the standard dilutions of TNF- $\alpha$ , IL-1 $\beta$ , IL-6, IL-10, IL-12, and VEGF cytokine was added to the control tube. A total of 50  $\mu$ L of each unknown sample was added to the appropriately labeled sample tubes. Subsequently, 50

$\mu$ L of TNF- $\alpha$ , IL-1 $\beta$ , IL-6, IL-10, IL-12, VEGF PE detection reagent was added to all the assay tubes followed by incubation in the dark for 3 hours at room temperature. Then, 1 mL of wash buffer was added to each tube and centrifuged at 200 g for 5 minutes, the supernatant discarded, and 300  $\mu$ L of wash buffer added for resuspending the bead pellet. The sample data was acquired on the flow cytometer and analyzed using FCAP Array software.

### ELISA

The plate was coated with 100  $\mu$ L/well of capture antibody, sealed, and incubated overnight at 4°C. The wells were aspirated and washed three times with wash buffer followed by locking with 200  $\mu$ L/well of diluent and incubation at room temperature for 1 hours. Then, 100  $\mu$ L/well of your samples is added to the appropriate wells, sealed, and incubated at room temperature for 2 hours. The process was then repeated for 3-5 washes. Subsequently, 100  $\mu$ L/well of detection antibody was added, the plate was sealed, and incubated at room temperature for 1 hour, followed by repeating for 3-5 washes. Finally, 100  $\mu$ L/well of diluted Avidin-HRP was added, the plate sealed, and incubated at room temperature for 30 minutes. The process was repeated for 5-7 washes followed by addition of 100  $\mu$ L/well of TMB. The plate was incubated at room temperature for 15 min, and then 50  $\mu$ L of stop solution was added and then the plate was estimated at 450 nm.

### Histopathological analysis

For histological preparations, the skin was fixed in 10% neutral buffered formalin and then embedded in paraffin. Skin tissues were sectioned in 5  $\mu$ m thickness slices for histopathological examination by hematoxy/eosin (HE), for collagen formation by Masson's Trichrome staining (Nanjing Jiancheng Bioengineering Institute, China) and for collagen type I/III by Sirius red staining (Beijing Zhngshan Jinqiao, China). The stained sections were observed with a microscope (zeiss, Germany).

### Immunohistochemistry

Paraffin-embedded tissues were dewaxed and rehydrated. After brief PBS wash, the slides were blocked with 10% normal donkey serum

# Huiyang Shengji Extract regulated macrophage phenotype transition

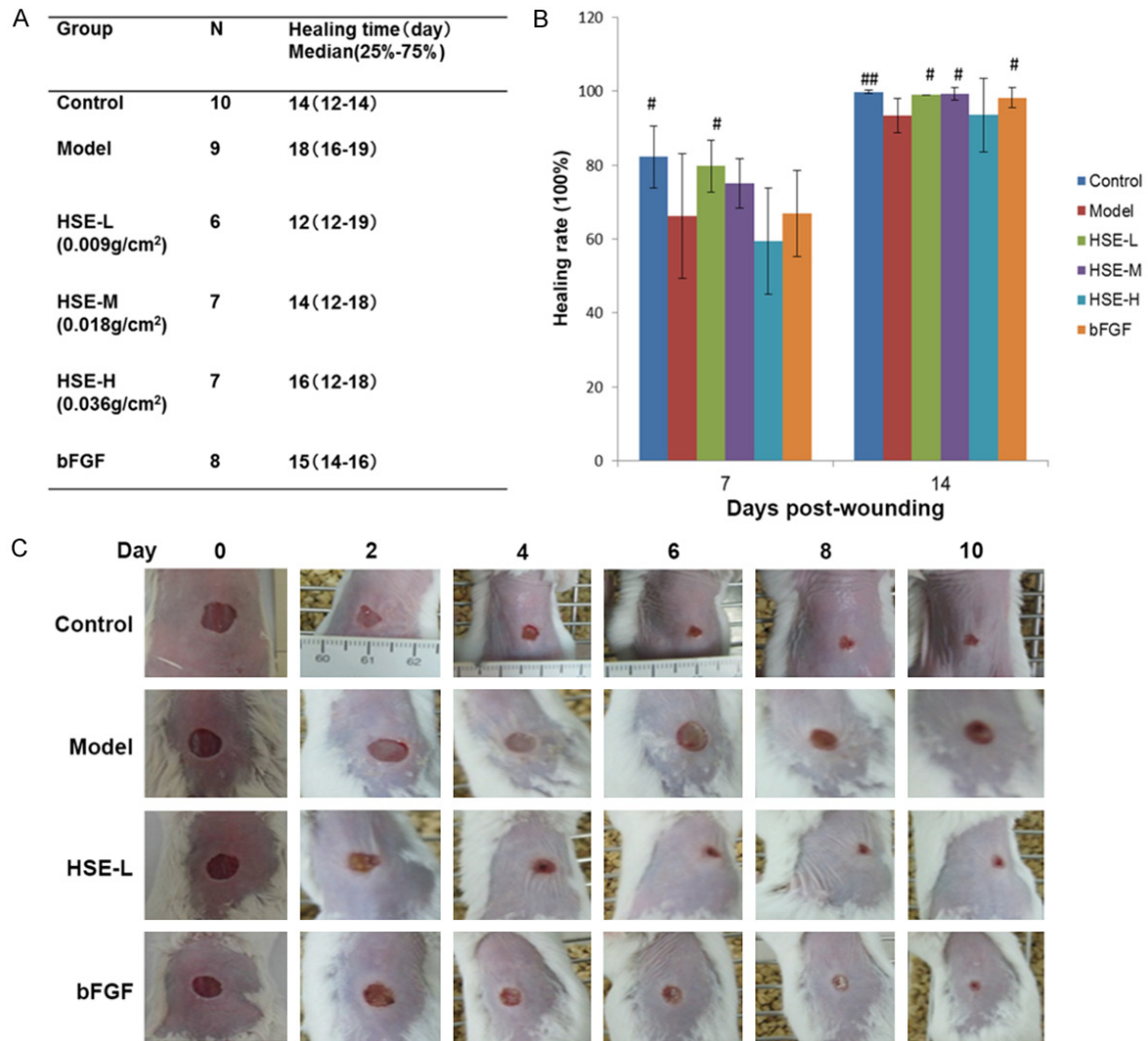


**Figure 3.** Effect of HSE administration on chronic wound healing of immunosuppressive mice induced by systemic hydrocortisone. A. HSE with various doses reduced the wound healing time. B. Wound healing rate of HSE-L groups was higher than that of the model group on days 7 and 14 ( $P < 0.05$ ). C. The wound's dynamic changes were observed by digital planimetry. \* $P < 0.05$ , \*\* $P < 0.01$  vs. model group.

for 30 minutes and then incubated with primary antibody against CD68 (1:200, Abcam, UK), iNOS (1:500, Abcam), and CD206 (1:500, Abcam). After an overnight incubation at 4°C, the slides were washed and incubated with TRITC-Affinipure donkey anti-mouse/rabbit IgG or 488-Affinipure donkey anti-rat IgG (Alexa Fluor; 1:500, Jackson ImmunoResearch) for 1 hour, then sealed with mounting medium with DAPI. The images were captured by a microscope using Axio Imager (Zeiss).

### Real time-RT-PCR

Total RNA was isolated with ultrapure RNA kit (CWBio. Co. Ltd., China). cDNA synthesis was

performed using HiFi-MMLV cDNA kit and UltraSYBR Mixture (with ROX) (CWBio). Primer sequences for targeted cDNA were listed in **Table 1**. PCR amplification parameters were: 95°C for 10 minutes, (95°C for 15 s, 60°C for 60 s) × 45 cycles, with ABI 7300 Real Time PCR. The relative quantitative analysis was carried out using  $2^{-\Delta\Delta Ct}$ .

### Western blot

The tissues were lysed in RIPA lysis buffer (Sainuobo, China). Protein concentrations of the lysates were determined using the Bicinchoninic Acid Kit for Protein Determination (Sainuobo). A total of 20 µg lysates were sub-

## Huiyang Shengji Extract regulated macrophage phenotype transition

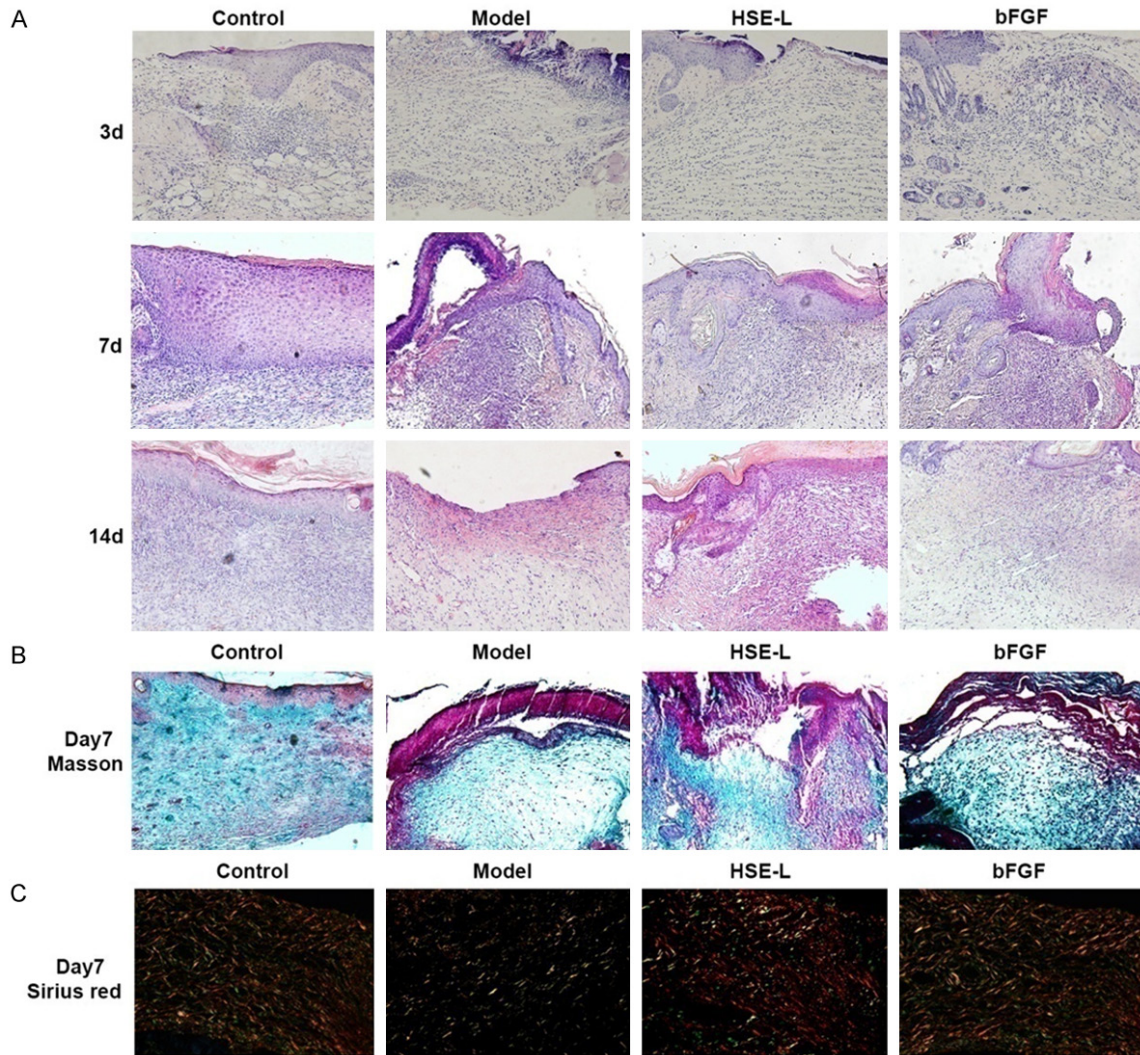


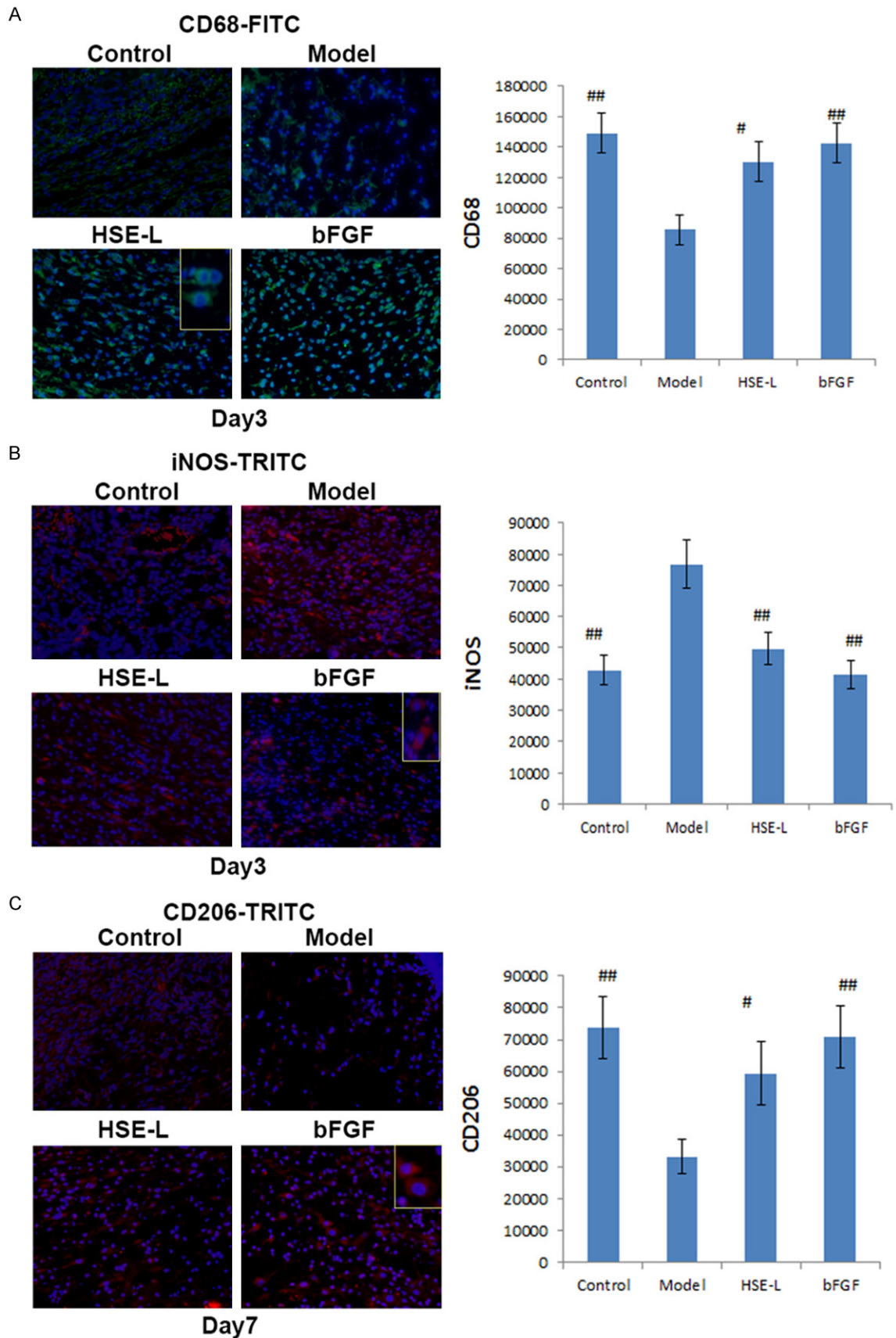
**Figure 4.** Morphological changes of the chronic wound in immunosuppressive mice after treated by HSE-L or bFGF (n=10). A. HE staining was conducted on days 3, 7, and 14 post-wounding. B. Masson staining showed newborn collagen tissue (blue) of the model group was less than the control group on day 7. Compared with the model group, the newborn collagen tissue of HSE-L and bFGF groups was excessive. C. Sirius red staining on day 7 was used to differentiate collagen type-I (green) and type-III (red or yellow). Sparse collagen of the model group was mainly collagen type-I and irregular arrangement, with little collagen type-III. Compared to the model group, excessive collagen type-III was seen with sparsely reticular arrangement for control/HSE-L and bFGF groups.

jected to a 10% SDS-PAGE analysis (Sainuobo) and transferred to nitrocellulose membrane (Millipore, Germany). The membranes were then blocked and incubated with primary antibodies against VEGF (1:4000, Abcam), TGF- $\beta$  (1:1000, Abcam), TNF- $\alpha$  (1:500, Abcam), and IL-6 (1:500, Abcam), overnight incubation at 4°C. GAPDH (1:20000, Tiandeyue, China) served as a loading control. Incubation of all primary antibodies was followed by incubation with an appropriate goat anti-rabbit IgG (H+L) HRP secondary antibody (1:20000). The immunoreactive bands were visualized by enhanced

chemiluminescence staining. The assay was carried out in at least three independent experiments.

### Statistical analysis

*In vitro* experiments were repeated at least three times. The data of healing time was expressed as median (25-75%), and the other results were presented as the mean  $\pm$  standard deviation (SD). The data analysis was performed using one-way ANOVA followed by the least significant difference (LSD) test. The dif-



## Huiyang Shengji Extract regulated macrophage phenotype transition

**Figure 5.** Macrophage number and a subpopulation of the chronic wound in immunosuppressive mice, after treatment with HSE-L, were analyzed by immunofluorescence method. The data are expressed as the mean  $\pm$  standard deviation (SD) of five mice per group. A. CD68-positive cells in the granulation tissue of HSE-treated mice were higher than the model group at day 3 after wounding ( $P<0.05$ ). B. In the granulation tissue of HSE-treated mice, iNOS-positive cells were decreased compared with the tissue from the model group at day 3 ( $P<0.01$ ). C. CD206-positive cells were increased in the granulation tissue of HSE-L and bFGF groups in comparison with the model group at day 7 ( $P<0.05$ ). # $P<0.05$ , ## $P<0.01$  vs. model group.

ferences were considered statistically significant when  $P<0.05$ . The data were analyzed using SPSS20.0.

### Results

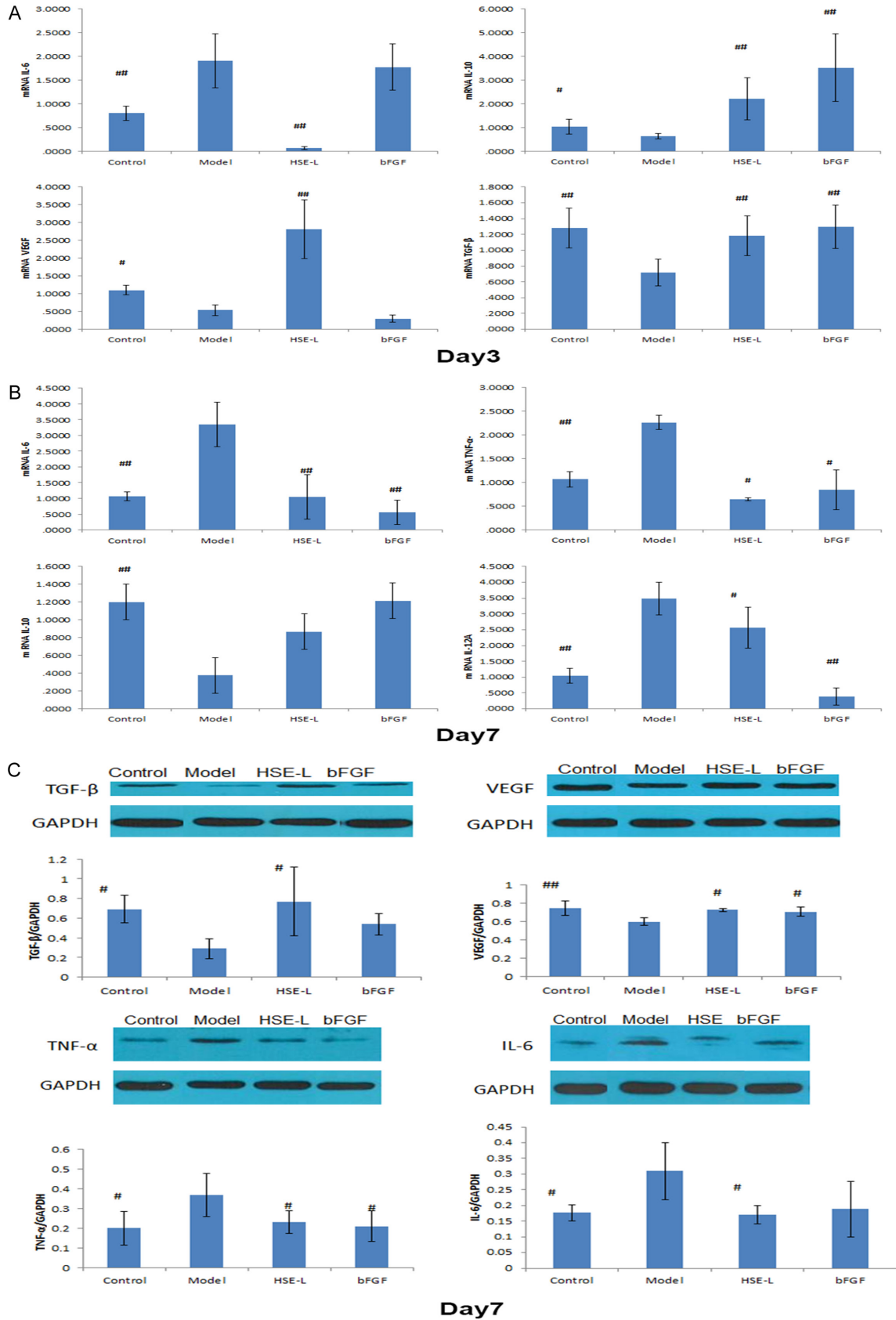
The role of HSE on delayed wound healing time and rate was elucidated through immunosuppressive mice. The wound healing time of control mice was 14 (12-14) days, of which the model group was prolonged up to 18 (16-19) days (**Figure 3A**). The wound healing time of the HSE groups with a low dose (HSE-L) was 12 (12-19) days, medium dose (HSE-M) 14 (12-18) days, and high dose (HSE-H) 16 (12-18) days, whereas, the bFGF group healed in 15 (14-16) days. The wound healing rate of the model group was lower than that of the control group on day 7 and 14 ( $P<0.01$ ,  $P<0.05$ ). The wound healing rate of the HSE-L groups was higher than that of the model group on day 7 and 14 ( $P<0.05$ ). Compared with the model group, the healing rate of HSE-H group showed no difference, of which bFGF and HSE-M groups were higher on day 14 ( $P<0.05$ , **Figure 3B**). These results revealed that HSE-L had an adequate effect on delayed wound of immunosuppressive mice, which was selected as the following experimental concentration of HSE. The wound dynamic changes were observed by digital planimetry (**Figure 3C**).

To elucidate the histological characteristics of delayed wound after treatment by HSE-L, HE staining was conducted on day 3, 7, and 14 post-wounding (**Figure 4A**). On day 3 post-wounding, the epithelial cells of the control group became thick and crawled from the edge of the wound to the bed of the wound, and more inflammatory cells were infiltrated. Compared with the control group, distinct inflammatory reaction and an apparent gap were seen on the bed of wound for the model group. Compared with the model group, more cells (many inflammatory cells and little repairing cells) were generated on the bed of wound of HSE-L and bFGF groups. On day 7 post wounding, newborn,

thickened, and intact epidermis was seen, with few infiltrating inflammatory cells on the wound of the control group. Distinct crusta, newly generated epidermis, and a large number of infiltrating inflammatory cells were seen on the wound of the model group. In the case of the HSE-L group, epidermis on the edge of wound thickened and extended to the center of the wound and new born granulation tissue growth was seen with few infiltrating inflammatory cells. The bFGF group also showed newborn and thickened epidermis on the edge of the wound, with granulation tissue growth. On day 14 post wounding, newborn compact granulation tissue of the control group was observed with excess collagenous fiber, whereas, the little collagenous fiber was seen in newborn granulation tissue of the model group. A large amount of the newborn fibroblast cells and blood capillaries were observed in the bed of wound for HSE-L group, whereas, newborn compact granulation tissue was seen for the bFGF group. Masson and Sirius red staining were conducted on day 7 post wounding. Masson staining showed newborn collagen tissue (blue) in the model group that was less than that of the control group. Compared with the model group, the newborn collagen tissue of the HSE-L and bFGF groups was higher (**Figure 4B**). Sirius red staining was used to differentiate collagen type-I (green) and type-III (red or yellow). The results showed sparse collagen in the model group that was mainly collagen type-I and irregular arrangement, with little collagen type-III. Compared to the model group, excess collagen type-III was observed with a sparse reticular arrangement for control/HSE-L and bFGF groups (**Figure 4C**).

To assess the number of macrophages on the wound, immunofluorescence analysis with an antibody to CD68 (the macrophage marker) was performed (**Figure 5A**). CD68-positive cells in the granulation tissue of HSE-L group were higher than in the model group at day 3 post-wounding. To assess the infiltrating macrophages subpopulation on the wound, iNOS (a

# Huiyang Shengji Extract regulated macrophage phenotype transition



## Huiyang Shengji Extract regulated macrophage phenotype transition

**Figure 6.** Effect of HSE-L on mRNA and protein expression of M1/M2 cytokines on the wound of immunosuppressive mice by quantitative real-time PCR and Western blot. A. HSE-L increased the level of VEGF/TGF- $\beta$  and IL-10 mRNA (M2 makers) and decreased the level of IL-6 mRNA (M1 markers) on day 3 post wounding ( $P<0.01$ ). B. HSE-L decreased the IL-6/IL-12A and TNF- $\alpha$  mRNA (M1 cytokines) on day 7 post wounding ( $P<0.05$ ) # $P<0.05$ , ## $P<0.01$  vs. model group. C. Compared with the model group, HSE-L increased VEGF and TGF- $\beta$  protein expression, decreased the protein expression of TNF- $\alpha$  and IL-6 (M1 cytokines) on day 7 post wounding. ( $P<0.05$ ) # $P<0.05$ , ## $P<0.01$  vs. model group.

marker of M1 macrophages) and CD206 (a marker of M2 macrophages) were examined. In the granulation tissue from HSE-L group, iNOS-positive cells were decreased at day 3 (**Figure 5B**), CD206-positive cells were increased at day 7 (**Figure 5C**) as compared with the wound of model group. BFGF groups also showed a similar result. The mRNA level and protein expression of M1/M2 type cytokines was detected on the wound of immunosuppressive mice. The result showed that HSE-L increased the level of VEGF/TGF- $\beta$  and IL-10 mRNA and decreased the level of IL-6 mRNA (M1 markers) on day 3 post wounding ( $P<0.01$ , **Figure 6A**). HSE-L decreased IL-6/IL-12A and TNF- $\alpha$  mRNA on day 7 post wounding ( $P<0.05$ , **Figure 6B**). Compared with the model group, HSE-L increased the VEGF and TGF- $\beta$  protein expression and decreased expression of TNF- $\alpha$  and IL-6 proteins on day 7 post wounding ( $P<0.05$ , **Figure 6C**) was observed.

*In vitro*, Thp-1 cells developed into macrophages after treatment with PMA for 24 h. These cells were non-polarized macrophages. The effect of HSE on the activity of macrophages was tested by CCK-8 assay after culture with macrophages for 24 h. The result did not show any HSE effect of the activity of macrophages when the concentration was below 0.0016 g/L (**Figure 7A**). The capability of macrophages phagocytosis also was detected by the neutral red method. HSE improved the macrophages phagocytosis from 0.000064 g/L to 0.008 g/L ( $P<0.05$ ). The chosen experimental concentration of HSE on macrophages was non-toxic, non-proliferative, and promoted the capability of macrophages phagocytosis. Thus, HSE-high/medium/low dose (0.0016/0.00032/0.000064 g/L) was selected for the downstream *in vitro* experiments for macrophages.

After being stimulated by LPS and IFN- $\gamma$  for 48 hours, the macrophages secreted a high level of TNF- $\alpha$ , IL-6, and IL-1 ( $P<0.01$ ), and a low level of IL-10, VEGF, and TGF- $\beta$  ( $P<0.01$ , **Figure 7B**).

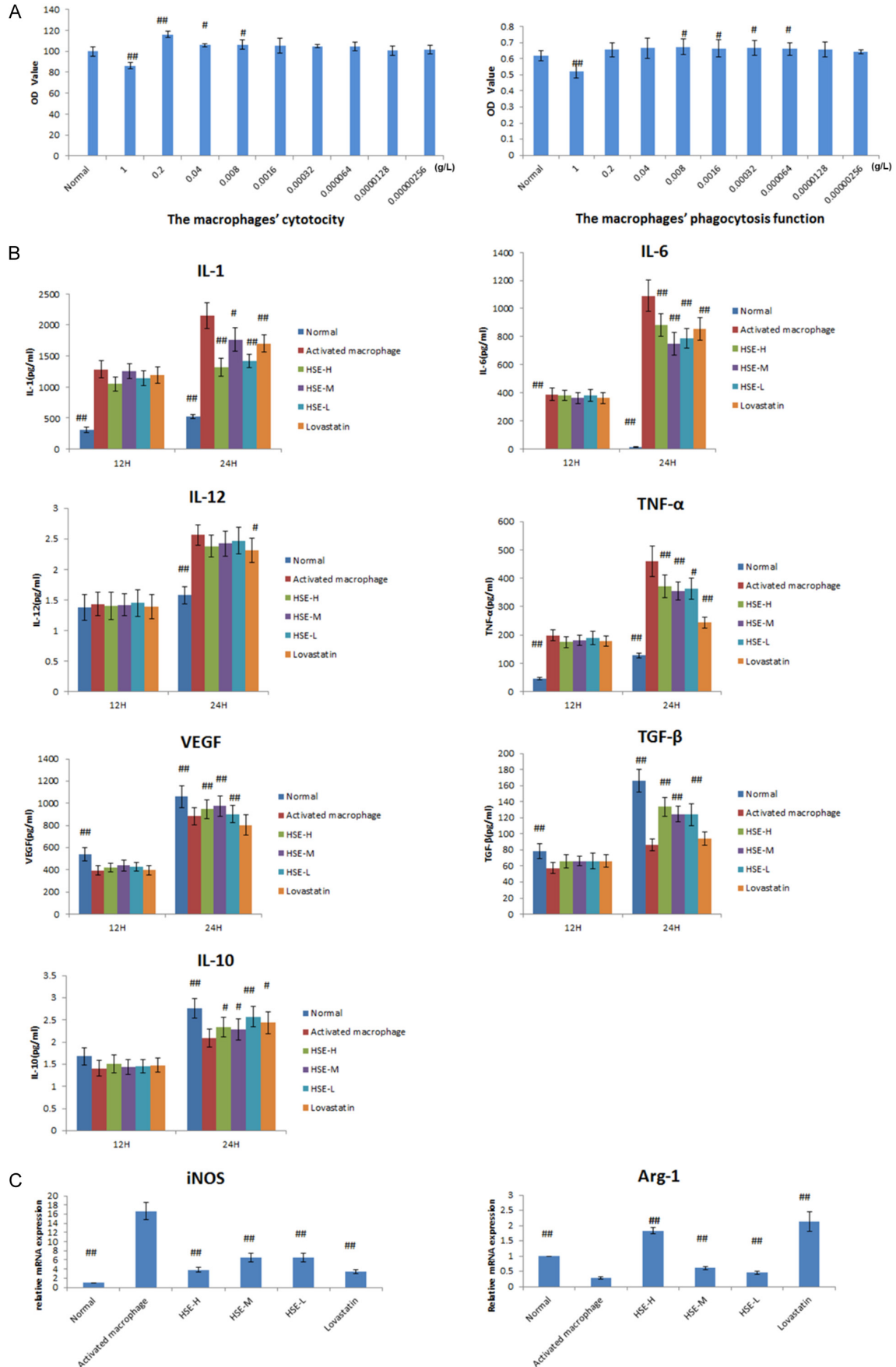
Thus, it indicated that macrophages became inflammatory activated macrophages. The results further showed that HSE inhibited the activated macrophages secreting TNF- $\alpha$ , IL-6, IL-1 ( $P<0.05$ ), and promoted those secreting VEGF, TGF- $\beta$ , and IL-10 at 24 hours ( $P<0.01$ ). Although IL-12 was also reduced but did not reach statistical significance, as well as, no difference between the activated macrophages and HSE groups for 12 hours ( $P>0.05$ ). We also detected mRNA expression of Arg-1 (M2 markers) and iNOS (M1 markers) of activated macrophages treated by HSE for 24 hours (**Figure 7C**). Compared with normal macrophages, Arg-1 mRNA level in activated macrophages was decreased significantly, and increased significantly following treatment with HSE, while iNOS mRNA level was increased significantly in activated macrophages and decreased significantly following treatment with HSE ( $P<0.01$ ). As a positive control, lovastatin also showed similar effects on activated macrophages, but mainly decreased iNOS mRNA, TNF- $\alpha$ , IL-6, IL-1, and IL-12 protein level, increased Arg-1 mRNA and IL-10 protein, and had no effect on VEGF and TGF- $\beta$  proteins.

### Discussion

Dysfunction of macrophage phenotypic transformation is known to be associated with diabetic wound, but little is known whether macrophage phenotype is related to delayed wound of immunosuppressive mice. The major conclusions of this study are that: i) an imbalance of macrophage phenotype contributed to impaired wound healing in immunosuppressive mice; ii) HSE promoted impaired wound healing by regulating the macrophage phenotype transition.

Because of the clinical complexity of chronic wounds, most animal models of chronic wounding failed to recapitulate the clinical features of chronic wounds, resulted from ischemia, diabetes, pressure, and reperfusion damage [4]. Since none of these models are optimal, we used animal models, which could be improved

# Huiyang Shengji Extract regulated macrophage phenotype transition



## Huiyang Shengji Extract regulated macrophage phenotype transition

**Figure 7.** Effect of HSE on activated macrophages' phenotype transition from M1 to M2 *in vitro*. A. Effect of HSE on cytotoxicity and phagocytosis capability of macrophages with CCK-8 assay and neutral red method. HSE had no effect on the activity of macrophages at a concentration  $<0.0016$  g/L. HSE improved the macrophage phagocytosis with concentration from  $0.000064$  g/L to  $0.008$  g/L ( $P<0.05$ ).  $##P<0.01$  vs. normal group. B. Effect of HSE on the inflammatory cytokines and growth factors secretion of activated macrophages with ELISA and Cytometric Beads Array HSE could decrease the level of TNF- $\alpha$ , IL-6, IL-12, IL-1 (M1 cytokines) and increase the level of IL-10, VEGF, and TGF- $\beta$  (M2 cytokines) in the activated macrophages. Data represent the mean  $\pm$  standard deviation (SD) from two replicated experiments.  $#P<0.05$ ,  $##P<0.01$  vs. activated macrophages group. C. Effect of HSE on the mRNA expression of Arg-1 (M2 markers) and iNOS (M1 markers) of activated macrophages for 24 h by RT-PCR. Compared with the normal macrophages, Arg-1 mRNA level in activated macrophages decreased significantly, and increased significantly following treatment with HSE and lovastatin. iNOS mRNA level increased significantly in activated macrophages and decreased significantly following treatment with HSE and lovastatin.  $#P<0.05$   $##P<0.01$  vs. activated macrophages group.

to aid better our search for pathological mechanisms and therapeutic targets to promote healing. In the present study, the excision wound model was immune-suppressive mice, which were treated by hydrocortisone (HC). Previous reports have shown stimulation with HC one week prior to wounding developed prolonged immune suppression, which significantly impaired the wound healing [20, 21]. Our results show that the wound healing process of the model group was prolonged compared with the control group. M1 cells (iNOS-positive) of the wound of the model mice were increased and the M2 cells (CD206-positive) decreased as compared to the control group. The results also showed an elevated mRNA and protein level of IL-6 and TNF- $\alpha$  and lower mRNA and protein level of VEGF/TGF- $\beta$  on the wound of the model mice. These suggest that an imbalance of macrophages phenotypes contribute to impaired wound healing in immunosuppressive mice.

An increasing number of studies revealed therapies that could promote chronic wound healing with a target to modulate macrophages phenotype, e.g Substance P, 21R-Dihydroxy-Docosahexaenoic acid, and TGF- $\beta$ 1 [23-25]. In the present study, our results demonstrate that HSE-L accelerated the delayed wound healing of immunosuppressive mice through shortening the healing time and elevating the healing rate, especially the effect appeared earlier than by bFGF. Histological observations showed that HSE relieved the inflammatory reaction and promoted the epithelial and granulation tissue growth, as well as, the collagen deposition of the delayed wound. Recruitment of macrophages to the granulation tissue plays a fundamental role in the wound healing [26]. The current study revealed the delayed wound healing in immune-suppressive mice correlated with attenuated recruitment of macrophages to the

granulation tissue. HSE and bFGF elevated the number of macrophages (CD68+ cells) on the wound, which indicated that HSE promoted the recruitment of macrophages to the wound tissue. The macrophages recruited into the wound tissue express properties of M1 polarization during the early stages of wound repair, and express properties of M2 polarization during the later stages of wound repair [27]. Our results further revealed that HSE decreased the expression of iNOS and IL-6 (M1 markers) on the wound tissue of immunosuppressive mice during the early stages, and increased the level of CD206, VEGF, and TGF- $\beta$  (M2 markers) in the wound tissue of immunosuppressive mice during granulation tissue formation stages (Figures 5, 6). These suggested that HSE strengthens the M2 marker expression and weakens the M1 marker expression. Therefore, HSE could promote macrophages polarization from pro-inflammatory M1 to pro-healing M2 macrophages on the wound of immunosuppressive mice. The role of bFGF in promoting wound healing has been recognized: accelerating healthy granulation and epithelialization, stimulating the extracellular matrix metabolism, growth, and movement of mesodermally derived cells and facilitating VEGF and FGF production [28-32]. In this study, bFGF showed the similar effects on delayed wound healing with HSE. However, the onset time was later than HSE. For example, VEGF mRNA level was up-regulated at day 3 for the HSE group, but not for the bFGF group. The wound healing rate of the HSE group was elevated at day 7, but not for the bFGF group.

To verify further whether HSE regulated the macrophages phenotype transition, we analyzed the level of M1/M2 markers of inflammatory activated macrophages *in vitro* treated by HSE. The results showed that HSE inhibited the

## Huiyang Shengji Extract regulated macrophage phenotype transition

inflammatory activated macrophages secreting M1 cytokines and promoted those secreting M2 cytokines, and also increased the level of Arg-1 mRNA, as well as, decreased iNOS mRNA level significantly. Lovastatin was used as positive control because it can modulate the macrophage function, which elicited the genetic program inhibiting M2 macrophage polarization, inducing apoptosis in macrophages through the Rac1/Cdc42/JNK pathway, thereby increasing the expression of CD14 in macrophages after inhibition of the cholesterol biosynthetic pathway [33-35]. Lovastatin also showed a similar effect on activated macrophages but exhibited no effect on VEGF and TGF- $\beta$  protein. HSE was better than lovastatin on the effect of macrophages polarization. Our findings revealed that HSE promoted the inflammatory activated macrophages polarizing to M2 macrophages from M1-polarized macrophages. These data support that HSE further promotes M1 macrophages transition to M2 macrophages.

HSE is an external herbal medicine for the non-healing wound in China; the active ingredients were of concern. Our research shows 21 chromatogram peaks that were identified by the UPLC/Q-TOF-MS<sup>E</sup> analysis (Figure 1). These peaks included: eleven types of components from chuanxiong rhizoma (chuanxiongol, ferulic acid, levistolide A, Z-ligustilide, Tokinolide B, E-ligustilide, Riligustilide, ysolecithin, enkyunolideP, n-Butylphthalide, SenkyunolideP), eight types of ginsenosides (Rd, Rf, Re, Rg1, Rg2, Rg3, Rb1, and Rh1-components of ginseng radix et rhizoma), cinnamic aldehyde (components of cinnamomi cortex), and lysophosphatidylcholine (component of cervi cornu pantotrichum). Rg1 improves lipopolysaccharide-induced acute lung injury by inhibiting inflammatory responses and modulating infiltration of M2 macrophages [36]. Rh1 potentiates dexamethasone's anti-inflammatory effects of chronic inflammatory disease [37]. Re inhibits TNF- $\alpha$  production [38]. The anti-inflammatory, related anti-oxidative, and MMP-9 inhibitory activities of 20(S)-Rg3, the major stereoisomeric form of Rg3, are confirmed in macrophages [39]. Cinnamic aldehyde decreased the NO, TNF- $\alpha$ , and PGE2 levels in the serum and decreased iNOS, COX-2, and NF- $\kappa$ B expressions in the Carr-induced paw edema [40, 41]. However, little is reported about the effect on

macrophage polarization of chuanxiong rhizoma's components, lysophosphatidylcholine, and cinnamic aldehyde.

Although the wound macrophages have been classified as either M1 or M2 macrophages, this simple dichotomous nomenclature does not adequately reflect the complex biology of macrophage subsets [25, 42]. The M2 macrophages are now further categorized into various subtypes that promote wound healing, immune-regulation, or resolution of inflammation [43]. However, the mechanisms of HSE on regulating the M1-to-M2 phenotypic switch during delayed wound healing remain to be elucidated. Our future work will also include screening out the core components of HSE.

### Conclusions

HC-induced immunosuppressive mice exhibited dysregulated macrophage phenotype transition function in the wound, which in turn resulted in impaired wound healing. HSE promoted the impaired wound healing of immunosuppressive mice through regulating macrophage phenotype transition from pro-inflammatory M1 phenotype to pro-healing M2 phenotype, aiming to make it change from inflammatory phase to proliferative stage. The macrophages *in vitro* also confirmed this conclusion. This is an underlying mechanism of HSE for the therapy of chronic non-healing wound.

### Acknowledgements

This work was supported by the National Natural Science Foundation of China (No. 81273768, 81403270, 81403409).

### Disclosure of conflict of interest

None.

**Address correspondence to:** Ping Li, Beijing Institute of TCM, Beijing Hospital of Traditional Chinese Medicine, Capital Medical University, Beijing, P. R. China. Tel: +86-13683313011; Fax: +86-21-6408-5875; E-mail: liping411@126.com

### References

- [1] Guest JF, Ayoub N, McIlwraith T, Uchegbu I, Gerrish A, Weidlich D, Vowden K, Vowden P. Health economic burden that wounds impose

## Huiyang Shengji Extract regulated macrophage phenotype transition

- on the National Health Service in the UK. *BMJ Open* 2015; 5: e009283.
- [2] Jiang Y, Huang S, Fu X, Liu H, Ran X, Lu S, Hu D, Li Q, Zhang H, Li Y, Wang R, Xie T, Cheng B, Wang L, Liu Y, Ye X, Han C, Chen H. Epidemiology of chronic cutaneous wounds in China. *Wound Repair Regen* 2011; 19: 181-8.
- [3] Bus SA, van Netten JJ. A shift in priority in diabetic foot care and research: 75% of foot ulcers are preventable. *Diabetes Metab Res Rev* 2016; 32 Suppl 1: 195-200.
- [4] Nunan R, Harding KG, Martin P. Clinical challenges of chronic wounds: searching for an optimal animal model to recapitulate their complexity. *Dis Model Mech* 2014; 7: 1205-13.
- [5] Dai MK, Li P, Liang YH, Wang YG, Yang HJ, Sheng X, et al. Analysis of matrix-metalloproteinases and their inhibitors in the skin wound fluids from ulcers of Yin and Yang syndromes. *Chinese Journal of Basic Medicine in Traditional Chinese Medicine* 2009; 15: 298-300.
- [6] Zhu CJ, Zhang ZH, Ma J, Li PC, Liu XZ, Yin Y, Tian Y. [Primary investigation on fumigation and moxibustion in treatment ulcer and sore of yin syndrome]. *Zhongguo Zhen Jiu* 2011; 31: 799-801.
- [7] Pukstad BS, Ryan L, Flo TH, Stenvik J, Moseley R, Harding K, Thomas DW, Espevik T. Non-healing is associated with persistent stimulation of the innate immune response in chronic venous leg ulcers. *J Dermatol Sci* 2010; 59: 115-22.
- [8] Mirza R, Koh TJ. Dysregulation of monocyte/macrophage phenotype in wounds of diabetic mice. *Cytokine* 2011; 56: 256-64.
- [9] Bartonicek J, Tucek M, Lunacek L. [Judet posterior approach to the scapula]. *Acta Chir Orthop Traumatol Cech* 2008; 75: 429-35.
- [10] Gurtner GC, Werner S, Barrandon Y, Longaker MT. Wound repair and regeneration. *Nature* 2008; 453: 314-21.
- [11] Mills CD. Anatomy of a discovery: m1 and m2 macrophages. *Front Immunol* 2015; 6: 212.
- [12] Khanna S, Biswas S, Shang Y, Collard E, Azad A, Kauh C, Bhasker V, Gordillo GM, Sen CK, Roy S. Macrophage dysfunction impairs resolution of inflammation in the wounds of diabetic mice. *PLoS One* 2010; 5: e9539.
- [13] Sindrilaru A, Peters T, Wieschalka S, Baican C, Baican A, Peter H, Hainzl A, Schatz S, Qi Y, Schlecht A, Weiss JM, Wlaschek M, Sunderkötter C, Scharffetter-Kochanek K. An unrestrained proinflammatory M1 macrophage population induced by iron impairs wound healing in humans and mice. *J Clin Invest* 2011; 121: 985-97.
- [14] Mirza RE, Fang MM, Ennis WJ, Koh TJ. Blocking interleukin-1beta induces a healing-associated wound macrophage phenotype and improves healing in type 2 diabetes. *Diabetes* 2013; 62: 2579-87.
- [15] Jetten N, Roumans N, Gijbels MJ, Romano A, Post MJ, de Winther MP, van der Hulst RR, Xanthoulea S. Wound administration of M2-polarized macrophages does not improve murine cutaneous healing responses. *PLoS One* 2014; 9: e102994.
- [16] Zhang QZ, Su WR, Shi SH, Wilder-Smith P, Xiang AP, Wong A, Nguyen AL, Kwon CW, Le AD. Human gingiva-derived mesenchymal stem cells elicit polarization of m2 macrophages and enhance cutaneous wound healing. *Stem Cells* 2010; 28: 1856-68.
- [17] Wang GY, Wang FS, Ding Y. A preliminary study on Huiyang Shengji Ointment to chronic skin ulcers of the morphological changes. *Chinese Medicine Herald* 2014; 11: 90-3.
- [18] Zhang Y, Wang F, Li P. Effects of Huiyang Shengji Gao on c-fos and c-myc expression of human fibroblasts derived from chronic ulcer margin skin. *Chinese Journal of Surgery of Integrated Traditional and Western Medicine* 2006; 12: 391-4.
- [19] Zhang Y, Li P, Wang F. Effects of Huiyang Shengji Gao on proliferation of human fibroblasts derived from normal and chronic ulcer-margin skin. *Chinese Journal of Pathophysiology* 2006; 22: 1808-10.
- [20] Gupta A, Jain GK, Raghubir R. A time course study for the development of an immunocompromised wound model, using hydrocortisone. *J Pharmacol Toxicol Methods* 1999; 41: 183-7.
- [21] Beck LS, DeGuzman L, Lee WP, Xu Y, Siegel MW, Amento EP. One systemic administration of transforming growth factor-beta 1 reverses age- or glucocorticoid-impaired wound healing. *J Clin Invest* 1993; 92: 2841-9.
- [22] Daigneault M, Preston JA, Marriott HM, Whyte MK, Dockrell DH. The identification of markers of macrophage differentiation in PMA-stimulated THP-1 cells and monocyte-derived macrophages. *PLoS One* 2010; 5: e8668.
- [23] Leal EC, Carvalho E, Tellechea A, Kafanas A, Tecilazich F, Kearney C, Kuchibhotla S, Auster ME, Kokkotou E, Mooney DJ, LoGerfo FW, Pradhan-Nabzdyk L, Veves A. Substance P promotes wound healing in diabetes by modulating inflammation and macrophage phenotype. *Am J Pathol* 2015; 185: 1638-48.
- [24] Tian H, Lu Y, Shah SP, Hong S. Autacoid 14S,21R-dihydroxy-docosahexaenoic acid counteracts diabetic impairment of macrophage prohealing functions. *Am J Pathol* 2011; 179: 1780-91.
- [25] Okizaki S, Ito Y, Hosono K, Oba K, Ohkubo H, Amano H, Shichiri M, Majima M. Suppressed recruitment of alternatively activated macrophages reduces TGF-β1 and impairs wound

## Huiyang Shengji Extract regulated macrophage phenotype transition

- healing in streptozotocin-induced diabetic mice. *Biomed Pharmacother* 2015; 70: 317-25.
- [26] Brancato SK, Albina JE. Wound macrophages as key regulators of repair: origin, phenotype, and function. *Am J Pathol* 2011; 178: 19-25.
- [27] Willenborg S, Lucas T, van Loo G, Knipper JA, Krieg T, Haase I, Brachvogel B, Hammerschmidt M, Nagy A, Ferrara N, Pasparakis M, Eming SA. CCR2 recruits an inflammatory macrophage subpopulation critical for angiogenesis in tissue repair. *Blood* 2012; 120: 613-25.
- [28] Yu A, Niiyama H, Kondo S, Yamamoto A, Suzuki R, Kuroyanagi Y. Wound dressing composed of hyaluronic acid and collagen containing EGF or bFGF: comparative culture study. *J Biomater Sci Polym Ed* 2013; 24: 1015-26.
- [29] McGee GS, Davidson JM, Buckley A, Sommer A, Woodward SC, Aquino AM, Barbour R, Demetriou AA. Recombinant basic fibroblast growth factor accelerates wound healing. *J Surg Res* 1988; 45: 145-53.
- [30] Matsumoto S, Tanaka R, Okada K, Arita K, Hyakusoku H, Miyamoto M, Tabata Y, Mizuno H. The effect of control-released basic fibroblast growth factor in wound healing: histological analyses and clinical application. *Plast Reconstr Surg Glob Open* 2013; 1: e44.
- [31] Marti-Carvajal AJ, Gluud C, Nicola S, Simancas-Racines D, Reveiz L, Oliva P, Cedeño-Taborda J. Growth factors for treating diabetic foot ulcers. *Cochrane Database Syst Rev* 2015; CD008548.
- [32] Barrientos S, Brem H, Stojadinovic O, Tomic-Canic M. Clinical application of growth factors and cytokines in wound healing. *Wound Repair Regen* 2014; 22: 569-78.
- [33] Mira E, Carmona-Rodriguez L, Tardaguila M, Azcoitia I, Gonzalez-Martin A, Almonacid L, Casas J, Fabriás G, Mañes S. A lovastatin-elicited genetic program inhibits M2 macrophage polarization and enhances T cell infiltration into spontaneous mouse mammary tumors. *Oncotarget* 2013; 4: 2288-301.
- [34] Liang SL, Liu H, Zhou A. Lovastatin-induced apoptosis in macrophages through the Rac1/Cdc42/JNK pathway. *J Immunol* 2006; 177: 651-6.
- [35] Frey T, De Maio A. Increased expression of CD14 in macrophages after inhibition of the cholesterol biosynthetic pathway by lovastatin. *Mol Med* 2007; 13: 592-604.
- [36] Bao S, Zou Y, Wang B, Li Y, Zhu J, Luo Y, Li J. Ginsenoside Rg1 improves lipopolysaccharide-induced acute lung injury by inhibiting inflammatory responses and modulating infiltration of M2 macrophages. *Int Immunopharmacol* 2015; 28: 429-34.
- [37] Li J, Du J, Liu D, Cheng B, Fang F, Weng L, Wang C, Ling C. Ginsenoside Rh1 potentiates dexamethasone's anti-inflammatory effects for chronic inflammatory disease by reversing dexamethasone-induced resistance. *Arthritis Res Ther* 2014; 16: R106.
- [38] Gao Y, Yang MF, Su YP, Jiang HM, You XJ, Yang YJ, Zhang HL. Ginsenoside Re reduces insulin resistance through activation of PPAR-gamma pathway and inhibition of TNF-alpha production. *J Ethnopharmacol* 2013; 147: 509-16.
- [39] Shin YM, Jung HJ, Choi WY, Lim CJ. Antioxidative, anti-inflammatory, and matrix metalloproteinase inhibitory activities of 20(S)-ginsenoside Rg3 in cultured mammalian cell lines. *Mol Biol Rep* 2013; 40: 269-79.
- [40] Gunawardena D, Karunaweera N, Lee S, van Der Kooy F, Harman DG, Raju R, Bennett L, Gyengesi E, Sucher NJ, Münch G. Anti-inflammatory activity of cinnamon (*C. zeylanicum* and *C. cassia*) extracts-identification of E-cinnamaldehyde and o-methoxy cinnamaldehyde as the most potent bioactive compounds. *Food Funct* 2015; 6: 910-9.
- [41] Liao JC, Deng JS, Chiu CS, Hou WC, Huang SS, Shie PH, Huang GJ. Anti-inflammatory activities of cinnamomum cassia constituents in vitro and in vivo. *Evid Based Complement Alternat Med* 2012; 2012: 429320.
- [42] Murray PJ, Allen JE, Biswas SK, Fisher EA, Gilroy DW, Goerdt S, Gordon S, Hamilton JA, Ivashkiv LB, Lawrence T, Locati M, Mantovani A, Martinez FO, Mege JL, Mosser DM, Natoli G, Saeij JP, Schultze JL, Shirey KA, Sica A, Suttles J, Udalova I, van Genderachter JA, Vogel SN, Wynn TA. Macrophage activation and polarization: nomenclature and experimental guidelines. *Immunity* 2014; 41: 14-20.
- [43] Mantovani A, Biswas SK, Galdiero MR, Sica A, Locati M. Macrophage plasticity and polarization in tissue repair and remodelling. *J Pathol* 2013; 229: 176-85.